

# Geomorphic Imprints of Active Tectonics of the Bikaner-Nagaur Petroliferous Rift Basin and its Surroundings (Western Rajasthan, India)

Mery Biswas<sup>1</sup>, Adrija Raha<sup>1</sup>, Soumyajit Mukherjee<sup>2\*</sup> and Vinit Shailesh Kotak<sup>3</sup>

<sup>1</sup>Department of Geography, Presidency University, 86/1 College Street, Kolkata - 700 073, India

<sup>2</sup>Department of Earth Sciences, Indian Institute of Technology Bombay, Powai, Mumbai - 400 076, India

<sup>3</sup>Department of Geology, K. J. Somaiya College of Science and Commerce, Vidyanagar, Vidya Vihar East, Ghatkopar East, Mumbai - 400 077, India

\*E-mail: smukherjee@iitb.ac.in, soumyajitm@gmail.com

Received: 8 March 2023 / Revised form Accepted: 1 July 2023

© 2024 Geological Society of India, Bengaluru, India

## ABSTRACT

Geology of sedimentary rift-basins require strong geomorphic input for a proper interpretation of active tectonics. Rift-related sedimentation took place in western Rajasthan of the Indian shield, which includes the Bikaner-Nagaur basin (BNB) and a few other adjacent basins. The sedimentation history of the BNB includes Proterozoic, Cambrian, Permo-Carboniferous and from Paleocene to the Recent. This study analyses river profiles with the best-fit curve ( $R^2$ ) model for the BNB and the surrounding regions. The research shows that the watershed 3 within the study area is most active tectonically, through which multiple faults and lineaments pass. Hypsometric Curves (HCs) of watersheds 1, 2 and 3 indicate that these watersheds are tectonically active. This inference is based on the concave profiles of HCs at the head, and convex profiles of HCs at the body and toe sections. Clustering of sixty segments (S) of the considered rivers based on linear-scale morphometric parameters, e.g., sinuosity index (SI), stream length gradient index (SL) and concavity ( $\theta$ ) enabled segment-wise comparison of river profiles with similar values. These segments were compared pair-wise, and Euclidean-based dissimilarity ( $d_R$ ) values were calculated between each such pair. The findings too imply that tectonic activeness exists in parts of watersheds 1, 2 and 3. The channel flow lines are controlled by faults/lineaments as per the micro-scale examination of the drainage network and faults/lineaments analysis. Under structural control, nine major geomorphic units emerged with distinct erosional surfaces, denudational hillocks, dissected hills and inselbergs. Detailed geomorphic map with micro-scale studies revealed a slope retreat process that resulted in landforms viz., pediment, pediment slope and active flood plains.

## INTRODUCTION

The geologic history of the state Rajasthan in western India covers the period from Early Archaean up to the Recent. This region has three major rift basins: Bikaner-Nagaur basin (BNB), Jaisalmer and the Barmer-Sanchor (Aiken and Brierley, 2013).

The BNB covers ~ 77,500 km<sup>2</sup> area (Ram, 2015) and spans parts of Jodhpur, Nagaur, Pali, Ajmer, Tonk, Jaipur and Sikar localities.

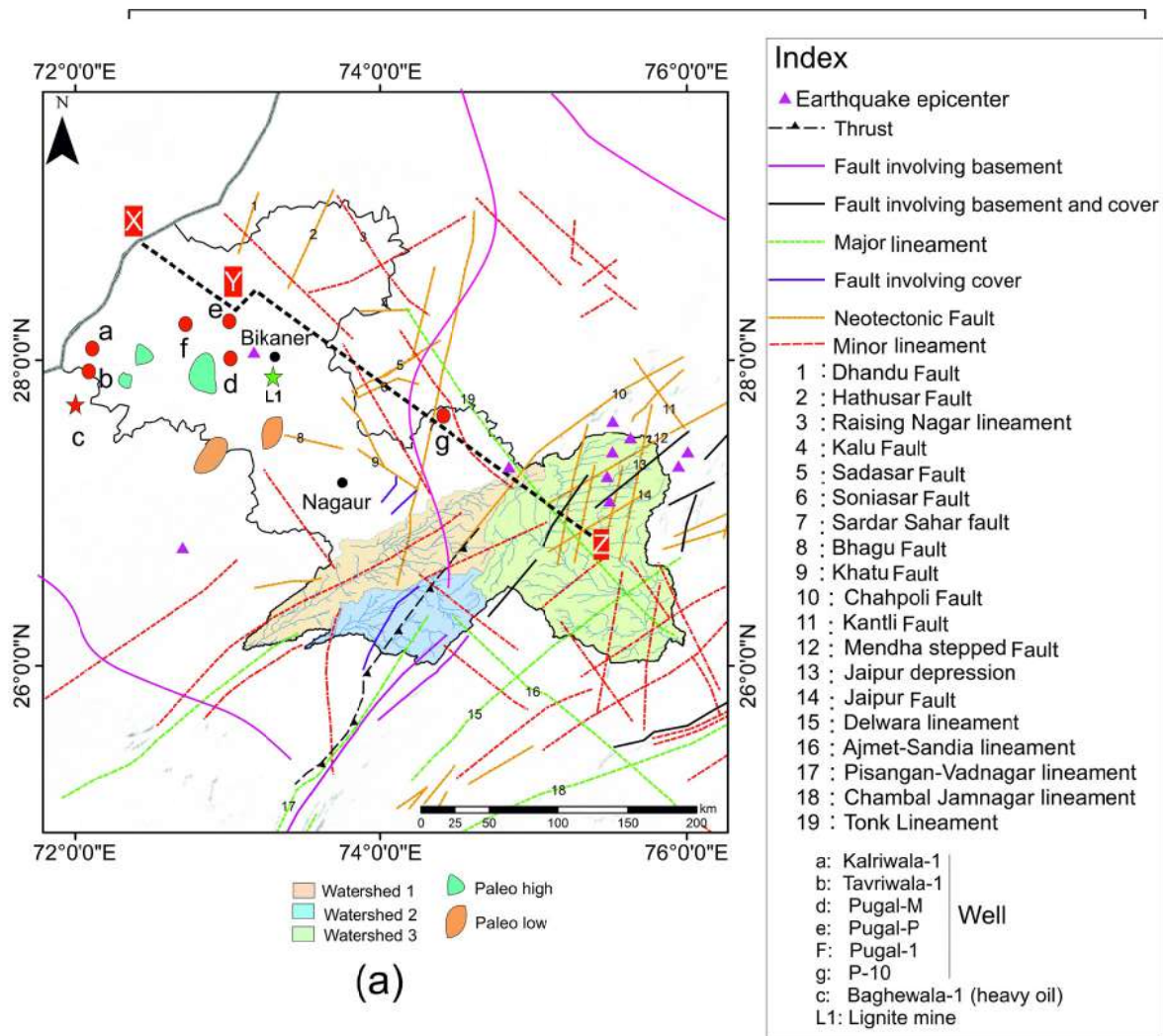
The basin is an extension of the Najd fault system of the Arabian plate (Agar, 1987; Luning et al., 2000). In the eastern region of Gondwanaland, the sinistral slip of the Najd faults in the Late Neoproterozoic created a succession of rift-grabens, including the Punjab rift and the BNB (Al-Husseini, 2000; Mandal et al., 2021). Neoproterozoic to Early Cambrian sedimentary succession makes up the majority of the pericratonic BNB (Prasad et al., 2010). The Marwar Supergroup deposited in the BNB is composed of the Jodhpur Group, Bilara and Hanseran Evaporite Group (HEG) and the Nagaur Group in the younging upward order.

The BNB lies on the rising flank of the Punjab platform in the Middle Indus basin in Pakistan (Fig. 1a) (Mandal et al., 2021). Marine evaporation reaching up to the BNB was constrained by the rocks of Infracambrian and Cambrian Eras. The Marwar Group of the BNB resembles the Huqf Group in south Oman (Yasin et al., 2022).

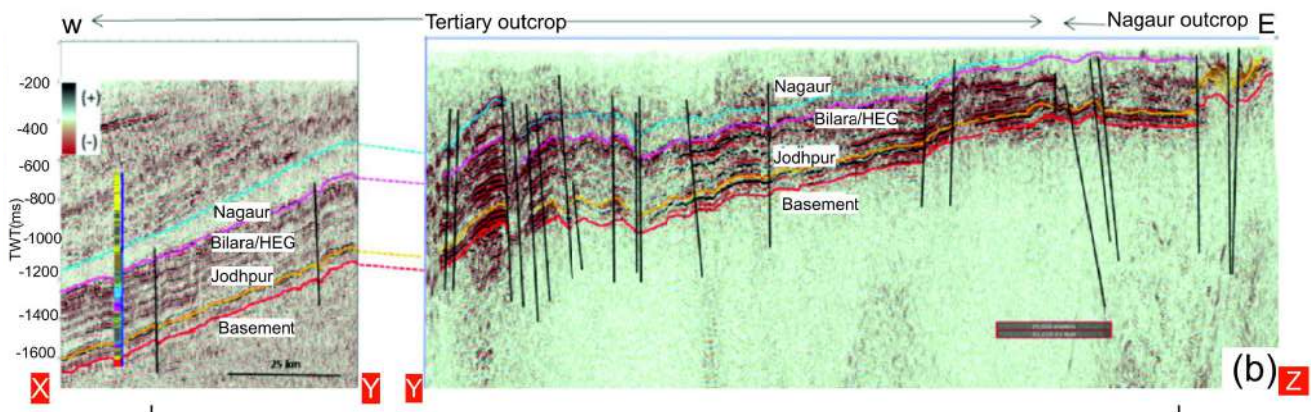
The elongated asymmetric BNB extends ~ 200 km in the E-W and has a maximum width of ~ 50 km (Rajak et al., 2019). As per the gravity data, the maximum thickness of the sediments is ~ 2-3 km and is surrounded by the Delhi-Aravalli fold belt in the east and south, the Delhi-Sargodha ridge in the northeast, and the Pokhran-Nachna high in the southwest (Das, 1988; Farooq et al., 2019). The basin merges with the Indus shelf in the north and northwest, where it deepens.

Morphotectonic analysis of rivers is useful for understanding tectonic geomorphology (Keller and Pinter, 1996, 2002). Longitudinal profiles of the river system record the recent tectonic deformation (Chen and Willet, 2016). Numerous researches on fluvial morphometry concentrate on high (relative) uplift rates, which is comparable with the Himalaya (Kirby and Whipple, 2001, 2012; Anand and Pradhan, 2019). Very few researches have worked on the slope-area relationships in less deformed regions such as the BNB (e.g., Marple and Talwani, 2000). In particular, only a few morphometric works exist on pericratonic and inter-cratonic basins worldwide (Table 1). Morphometric investigations of watersheds in and around the BNB (Fig. 1b) has so far remained a due.

The main objective of this research is to perform a morphotectonic analysis of the three watersheds located in the south and southeast of the BNB to understand (i) the tectonic prioritization of the watersheds in response to the channel quantification, and (ii) morphologic indications of active tectonics.



(a)



(b)

**Fig. 1. (a)** Location of the Bikaner-Nagaur basin (BNB) in Rajasthan. Faults and lineaments in BNB have been compiled from previous literature (Zutshi et al., 1997; Roy, 2006; Bhu et al., 2014; Wadhawan, 2018; Kumar et al., 2020). No data is available in the world stress map from the BNB area. Oil fields plotted from Raju et al. (2014) and Yasin et al. (2022). **(b)** Seismic profiles X-Y and Y-Z show several sub-surface faults near the oil fields and watershed 3 where horst-graben structures are found. Reproduced from Mandal et al. (2021).

## STUDY AREA

We performed morphotectonics on the three delineated watersheds in the south and southeast parts of the BNB using remote sensing and Geographical Information System (GIS) based methods (Fig. 1a). BNB is mostly covered with dunes and at many places no drainages exist (<https://earthquake.usgs.gov/earthquakes/search/> (Accessed on 28-Jan-2023)). The area surrounding BNB is covered by a huge semi-desert area that lacks significant surface water catchment characteristics. The cumulative area of the three considered watersheds is ~ 27,187 km<sup>2</sup>.

## GEOLOGY AND TECTONICS

The Malani Igneous Suite and the Delhi metamorphics comprise of a Precambrian basement with shallow elongated BNB (Singh et al., 2017a; Singh et al., 2020). The Delhi-Sargodha subsurface ridge, the Aravallis, and the Jodhpur-Pokhran-Chottan-Malani Ridge surround this basin. The basin's northern and southern boundaries characterize the E-W trending faults, while the basement highs occur at Dulmera and Suratgarh (Kumar and Pandit, 2020).

The Malani rocks, which emerged as fissure eruptions and formed

**Table 1.** Review of morphometric analysis in peri-cratonic and inter-cratonic basins

Authors	Terrain	Country	Approach	Conclusions
Kothyari and Rastogi (2013)	Upper Narmada valley	India	Through the application of tectonic geomorphometric parameters, e.g., stream length gradient index SL, asymmetry factor, transverse-topographic symmetry, and valley floor height ratio, the imprint of tectonism has been assessed. Different segments of the upper Narmada river basin under the influence of the active Son-Narmada Fault (SNF) zones in central Peninsular India have been examined.	Shahpuri-Mandla and Jabalpur-Narsihapur segments in the SNF zone are active, which uplifted the Narmada river basin. It has also been confirmed by the morphometric indices and the drainage pattern.
Kale et al. (2014)	Kaveri river drainage, cratonic Peninsular India	India	The middle reaches of the Kaveri river exhibit youthful characters. By analyzing longitudinal profiles, morphotectonic indices of active tectonics and fluvial records, the tectonic controls on this cratonic river were assessed. Index of Active Tectonics was computed.	Tectonic controls and differential erosion are exemplified. Due to the Kaveri river's rapid incision, tributaries experienced erosion. Numerous knickpoints, deep and narrow gorges hanging valleys, and past earthquake events show that this region is presently deforming.
Gandhi et al. (2015)	Southwestern Saurashtra, western India	India	Several geomorphic indices e.g., longitudinal river profile, stream length-gradient index, valley floor width-height ratio, asymmetry factor, transverse topography asymmetry, elongation ratio and pseudo-hypsometric integral have been used to identify the spatial variation in neotectonic activity.	Quantitative morphometric approach enabled dividing the study area into three zones based on the degree of neotectonic activity
Prakash et al. (2016)	Jamini River basin, Bundelkhand Craton, Central India	India	The analyses of the asymmetry factor, ruggedness number, basin relief, gradient, basin elongation ratio, drainage density analysis, and drainage pattern for each drainage basin using remote sensing and GIS techniques.	Impact of tectonic activity on the development of the watersheds studied.
Kothyari et al. (2018)	Kachchh rift basin, Western India	India	27 sub-watersheds were delineated on which few morpho-tectonic parameters e.g., stream length-gradient Index (SL), steepness index (Ks), hypso-metric integral (HI), asymmetric factor (AF) and Basin Shape (BS) have been applied. Based on results obtained from the selected parameters, relative index of active tectonics (RIAT) was estimated.	Geomorphic analyses from the SL, KS and RIAT distribution was made to confirm the tectonic activeness of the study area. The area's tectonic activity is further supported by the steepening of the river gradient as per the SL and KS.
Kanhaiya et al. (2019)	Dongar river basin, Son valley, central India	India	Several morphometric parameters were applied on the river basins e.g., stream length ratio, bifurcation ratio, relief ratio, elongation ratio, drainage density, stream frequency, form factor, circularity ratio, length of overland flow, ruggedness number, and the Melton ruggedness ratio.	Drainage pattern was shaped by tectonics and structures. Secondary deformations in the basin has been identified, which are due to the palaeo-seismic activity in the recent past.
Bhatt et al. (2020)	Pahuj catchment basin, central India	India	Morphometric analyses are conducted to comprehend landform processes as well as the physical and erosional characteristics of the basin's soil.	Less active tectonics was deciphered from the drainage pattern of basin catchments flowing through a terrain of diverse lithology and structures. Drainage lines are lineament and fault-controlled.
Solanki et al., (2021)	Shetrunji river, western India	India	The tectono-morphology of the river basin is examined in order to identify the neotectonic signatures through in-depth analyses of the landforms and drainage pattern.	The basin is neotectonically active. This is indicated by unpaired strath terraces, entrenched meandering, development of ravine surfaces, deflection of streams, knick points, straight courses, and narrow valleys/gorges.
Bragança et al., (2021)	Cotovelo river basin, Middle to Upper Proterozoic western foreland basin of the São Francisco craton, northwestern Minas Gerais	South-eastern Brazil	To understand the tectonic imprint on the subwatersheds several morphotectonic parameters were applied.	Morphology of the terrain was under the structural influence of recent, low-rate tectonic activity.
Siahaan et al., (2022)	Krueng Raya watershed, Aceh Besar, Indonesia	Indonesia	The geomorphometric variables were calculated on basin-scale (drainage density, stream frequency, circularity ratio and elongation ratio), as well as on linear-scale (bifurcation ratio and stream length ratio).	Narrow deformed elongated shape of the river basins with rough texture is deciphered.
Biswas et al. (this work)	Bikaner-Nagaur Basin and surroundings, western Rajasthan	India	Linear parameters- SL, SI and $\lambda$ , were treated segment-wise.	Well linked parameters in segments are concluded to be structurally and tectonically controlled.

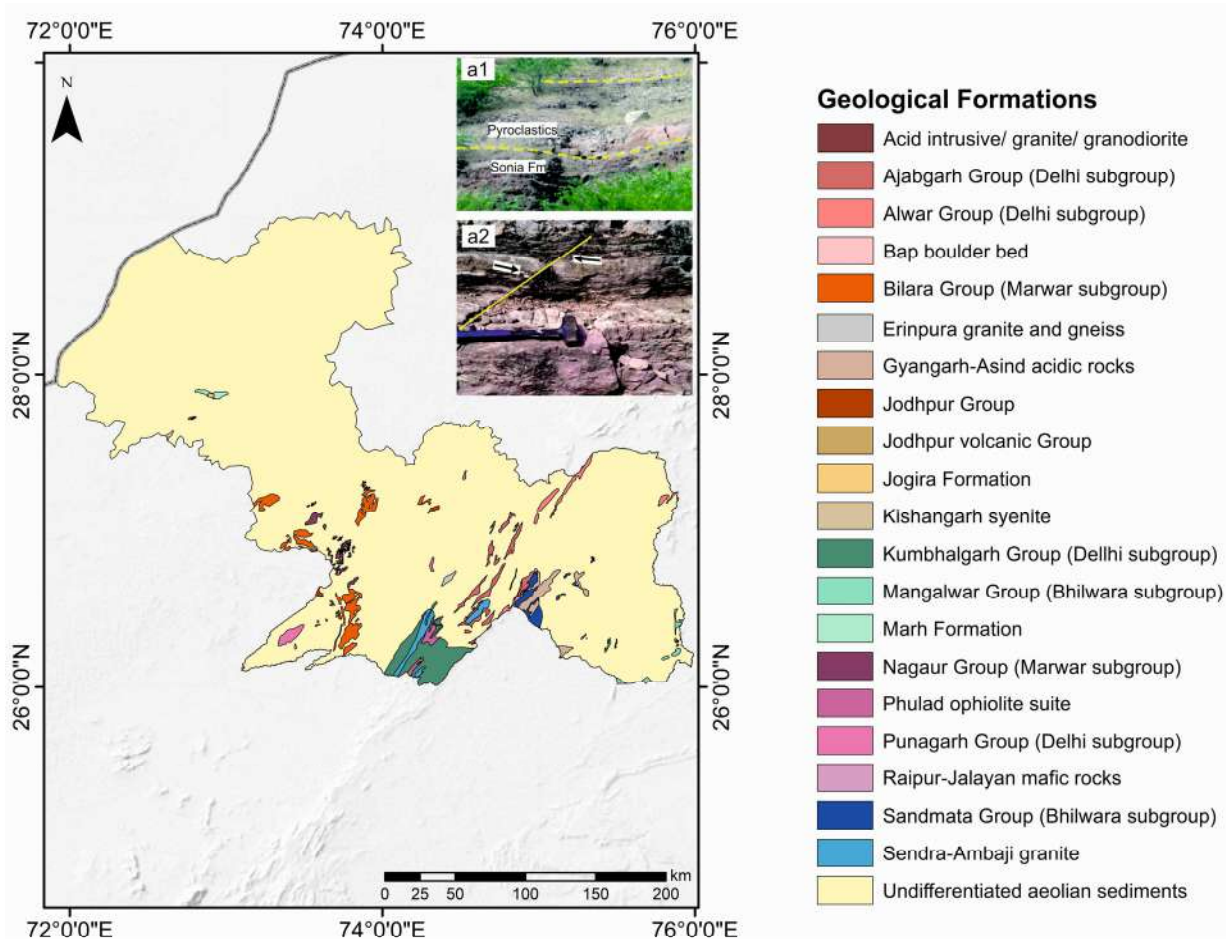


**Fig. 2.** Geologic formations of the Bikaner-Nagaur basin (BNB) (<https://bhukosh.gsi.gov.in/Bhukosh/Public> (Accessed on 15-Jan-2023)). (a1) Outcrop of the calcareous tuff at Chhoti Khatu village, Nagaur. (a2) A close-up view of the slipped tuff layer. Reproduced from George (2020).

deep tectonic structures along NNE-SSW, occurred next. Volcanic activities represented by Malani rhyolites ( $745 \pm 10$  Ma) and the Jalore Granite ( $600 \pm 70$  Ma) are related to the development of the BNB (Rasheed et al., 2011). (Fig. 2)

Das (1988) delineated several regional faults and related structures in the Delhi Supergroup rocks north of Jaipur. These NW-SE and NE-SW conjugate structures induced rotation and strike-slip movement. Sadasar Fault (SF) trends N-S to NNE-SSW and the slip component exceeds 400 m in the west as recorded in the Quaternary deposits (Kumar et al., 2005; Mandal et al., 2021). SF (and different parts of BNB) has been active in recent past due to recurring seismicity (Kumar and Pandit, 2020; Table 2). This fault is inferred to be active in the context of recent earthquake events (Internet ref-1). Repositories 1 and 2 present the stratigraphy of the BNB. The Bouguer anomaly

**Table 2.** Recent seismic activities in the study area (Internet ref-1; Kumar and Pandit, 2020)

Sl. no.	Location (degree)	Magnitude (Mb)	Year
1	28.1573 N / 73.1834 E	4	2019
2	27.5 N / 75.6 E	3.4	2018
3	27.0 N / 75.1 E	3.5	2016
4	27.1 N / 75.5 E	3.8	2016
5	27.3767 N/75.493 E	4	2015
6	27.264N / 75.491 E	3.6	2013
7	27.5N / 75.6° E	3	2011
8	27.38 N / 75.98 E	4.4	2003
9	26.816 N / 72.61 E	3.5	1996

pattern shows a gravity low near the BNB (Zutshi et al., 1997) (Figs. 1, 2 of Repository 1).

Figure 1a presents the faults and lineaments of the study area. The lineaments of Rajasthan have been divided into two groups (Narula et al., 2000): (i) those generated as new features cutting across all rock strata, and (ii) those formed as the reactivated Precambrian structure. Tertiary and Quaternary strata are sheared / faulted in the Bikaner-Ganganagar area (Kumar and Pandit, 2020). The reason of plotting all faults and lineaments delineated by previous authors in figure 1a is to find out whether they are confined to any specific domain. Where weak planes interacted, pull-apart basins were generated along curved strike-slip faults. The salt lake Sambhar is an example of such a basin (Kumar and Pandit, 2020, Fig. 1b). Major lineaments in Rajasthan run for > 300 km and crosscut Archean to Cenozoic strata. Most of these lineaments are interbasinal (Bakliwal and Ramasamy, 1987; Zutshi et al., 1997). These lineaments trend NNE-SSW, ENE-WSW and NW-SE. Repository 3 reviews these lineaments.

Several minor lineaments in the BNB (Fig. 1a) are the manifestations of lithologic contacts, folds' axial planar fractures, faults, dykes and joints (Bakliwal and Ramasamy, 1987; Bhola et al., 2004). These lineaments are predominantly tectonic features in the Aravalli, Delhi and Vindhyan Supergroup of rocks. The seismic sections along X-Y and Y-Z (Mandal et al., 2021) indicate the tectonic activity (Fig. 1b).

#### DATA SET AND METHODS

Shuttle Radar Topographic Mission (SRTM) Digital Elevation Model (DEM, acquired on 11-Feb-2000, published on 23-Sept-2014)

with 30 m spatial resolution has been used to extract drainage, delineate and analyze watersheds and calculate morphometric indices. The data does not contain cloud cover; hence atmospheric correction was not needed. To extract the stream network, hydrological tool of ArcGIS 10.4 is used. Slope directions have been deduced from each pixel to its eight-neighbour pixels. Watershed boundaries were delineated by applying discrete flow angles and single flow direction. Watersheds were delineated using pour/outlet points in ArcGIS 10.4 (2016) platform.

The master stream was extracted from the drainage network for the longitudinal river profile analysis. Sinuosity index (SI), stream length gradient index (SL) and concavity index ( $\theta$ ) were calculated for each segment (S).

### Longitudinal River Profile Analysis

Recent tectonic activities affect geomorphic/river systems. Long profile denotes the break of slope and formation of knick points due to tectonics and lithology from source to mouth.

The linear function is given by

$$y = ax + b \quad (\text{eqn 1})$$

The logarithmic function is presented as follows.

$$y = a \ln x + b \quad (\text{eqn 2})$$

Here  $y$  is the elevation ( $H/H_0$ ;  $H$ : elevation of each point,  $H_0$ : elevation of the source),  $x$  is the length of the river ( $L/L_0$ ;  $L$ : distance of the point from the source,  $L_0$ : total length of the stream) and  $a$ ,  $b$ : coefficients derived independently from each profile. The  $R^2$  value determines the best fit. The curve with the highest  $R^2$  value is the best-fit curve. Drainage lines and watersheds are extracted from SRTM using the ArcGIS 10.4.

Longitudinal profiles of a river system in a particular location are

commonly used to monitor the evolution of tectonic deformation (Cyr et al., 2014; Chen and Willet, 2016). As the longitudinal profiles of the river preserve information about the landscape evolution, any anomalies or abrupt changes in river gradients within the longitudinal profiles suggest tectonic events (Bhattarai et al., 2017; Han et al., 2017). Longitudinal river profiles can be classified into concave or convex types based on the relationship between the river incision and bedrock uplift. Under a steady-state condition, where vertical erosion equals the uplift amount, the longitudinal profile is concave upward. When the uplift exceeds the river incision, the longitudinal profile is convex (Ambili and Narayana, 2014).

The coefficient of assessment establishes the degree of fit ( $R^2$ ). The curve with the highest  $R^2$  value is the best-fit curve. Long profiles have low degrees of concavity. Therefore, the  $R^2$  value of linear function is highest amongst linear, exponential, logarithmic and power relations (Lee and Tsai, 2009).

The longitudinal profile of each watershed was divided into 20 segments of equal lengths (Fig. 3). SI and SL are plotted in the long profiles with lineaments and faults to assess the tectonic correlation along the channel. Leopold and Miller (1964) derived the formula for the SI:

$$SI = \frac{L_{cmax}}{L_R} \quad (\text{eqn 3})$$

Here  $L_{cmax}$ : mid channel length and  $L_R$ : straight length. SI indicates whether a river is sinuous, straight or meandering.

SL points out topographic breaks by defining the change in stream slope along a longitudinal river profile. The index is sensitive to variations in channel slope, which enables evaluation of the relationships between tectonic activity, rock resistance and topography (Keller and Pinter, 2002). A sharp lithologic variation and/or differential

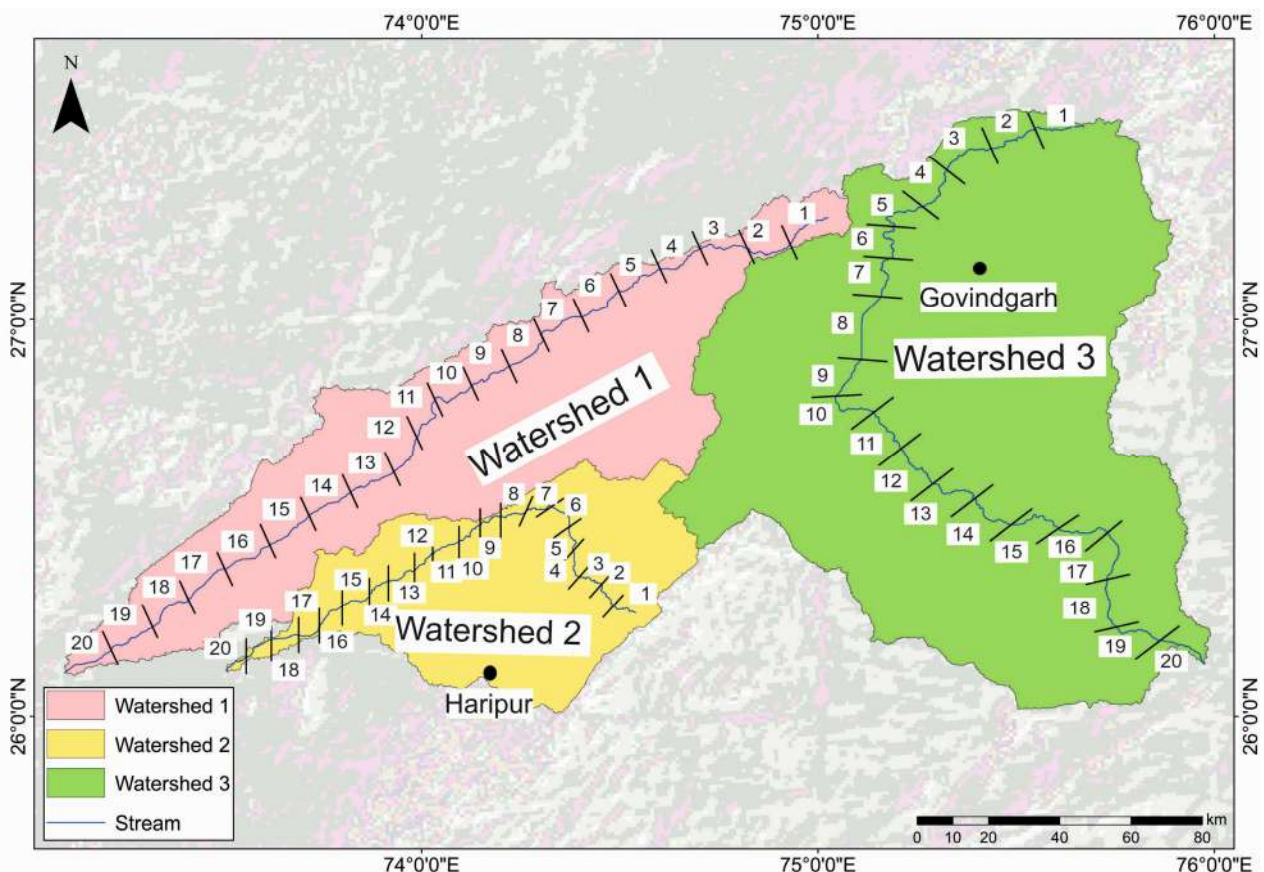


**Fig. 3.** Map of the study area with three watersheds delineated using ArcGIS 10.4. Twenty segments are marked from each master stream.

uplift across active structure are frequently connected with an abrupt change in SL along the river (Strahler, 1952; Hack, 1957, 1973; Seeber and Gornitz, 1983; Keller and Pinter, 2002; Whittaker et al., 2007).

SL is calculated using the formula (Hack, 1973; Keller and Pinter, 2002):

$$SL = \frac{\Delta H}{\Delta L} \times L \quad (\text{eqn 4})$$

Here  $\Delta H/\Delta L$ : gradient of the particular segment, and L: length of the stream from the midpoint of the segment to the highest point upstream of the river.

### Concavity index ( $\theta$ )

The parameter  $\theta$  primarily reflects the hydrology of the basin and the dominant erosion mechanism, while rock strength, channel bed material, runoff and sediment load influence the steepness. Tectonics, climate and base level change influence  $\theta$  (Zaprowski et al., 2005). Following Wobus et al. (2006) and Whipple et al. (2007),  $\theta$  is calculated as follows:

$$\theta = \frac{1}{S_2 - S_1} \Delta E \quad (\text{eqn 5})$$

Here  $S_1$ : channel slope prior to disturbance,  $S_2$ : channel slope after disturbance (e.g. due to a change in incision rate E), and  $\Delta E$ : difference between the incision rate before and after disturbance.

As per Lee and Tsai (2009), low  $\theta$  ( $< 0.4$ ) are often linked to knickpoints and are associated with either short, steep drainage impacted by debris flow or a downstream increase in incision rate or rock strength. Moderate  $\theta$  (0.4-0.7) indicates actively uplifting bedrock channels in a homogeneous rock, which undergoes (near) equal uplift rate. High  $\theta$  (0.7-1.0) indicates low rate of rock uplift at the downstream locations. Extreme  $\theta$ , either  $< 0$  or  $> 1$ , indicate a transition from incision to depositional conditions.

### Hypsometric Curves (HCs)

HC represents the distribution of a basin's area with regard to altitude (Strahler, 1952). HC characterizes basin's topography (Perez-Pena et al., 2009). It can be employed to unravel the interrelationship between tectonics, geomorphic processes and basin topography (Stepančikova et al., 2008). HCs were analysed using the percentage approach with the ratios (h/H) and (a/A) (Strahler, 1952; Anand and Pradhan, 2019; Biswas et al., 2022a,b). Plotting the relative area (a/A) on the abscissa (x-axis) and the relative elevation (h/H) on the ordinate (y-axis) yields the HC.

### Cluster Analysis of River Profiles

To comprehend the recent tectonics of an area, several methods have been applied on river networks. These methods generally consider that the base rock is homogeneous. However, due to changes in uplift rate, rock strength, climate and geomorphic processes, the landscape is heterogeneous (Clubb et al., 2019). In such a case, Clubb et al. (2019) suggested clustering the river profiles having similar morphologies so that tectonic, climatic or lithologic controls can be distinguished. Table 3 reviews clustering approaches made in geomorphic research.

Clustering can discriminate signals (grouping signals) from noise (source signals). This technique works on unsupervised classification. Therefore, no prior assumptions are needed. This enables a better research outcome from the heterogeneous landscapes. In this study, hierarchical clustering is performed on the river segments. The segments are clustered based on the degree of similarities of different channel segments. Most similar or dissimilar river segments are clustered first. Clusters of river segments that are less similar or

dissimilar are clustered later (dendrogram in Table 1 of Repository 4).

Three parameters (SL, SI and  $\theta$ ) were used to segregate the river segments and were numbered from 1 to 60 for clustering. Here segments 1-20 come from watersheds 1, 21-40 from watershed 2 and the remainder from watershed 3. The river segments were selected as per the nodes of interest. These parameters are user-defined and can be changed based on the data used and the area of interest.

Each segment was compared with the neighbouring segments to determine the degree of similarity using the Euclidean-based dissimilarity method. This was performed using the formula:

$$d_R = (\sqrt{\sum_{i=0}^n (X_i - Y_i)}) / n \quad (\text{eqn 6})$$

(eqn 6; Clubb et al., 2019)

Here  $d_R$ : Euclidean-based dissimilarity,  $X_i$ : distance between the segments,  $Y_i$ : difference of the steepness index between the pair of profiles, n: number of segments, and i: element in the array. Hierarchical clustering was done using the  $d_R$  values in the SPSS software (version 26, 2019) using the Ward's / minimum variance method. A dendrogram is prepared to demonstrate the relation of each segment to the other (Fig. 2 of Repository 1).

## RESULTS

To analyse the tectonic control on the evolution of drainage basins, longitudinal profiles, SI, SL and  $\theta$  were calculated for the master streams of each watershed. In watersheds 1 and 2, rivers mostly flow towards SW. River flows towards SE in watershed 3. Streams in the watersheds 1 and 3 are fourth order and those in the watershed 2 are third order. In watershed 1, tributaries join at right-angle forming rectangular drainage pattern (Fig. 3 of Repository 1). This pattern is controlled by hitherto unnamed N-S striking faults. The master stream in watershed 1 strongly follows the NNE-SSW trending unnamed lineament (Fig. 1a). Drainage lines in watershed 2 form complex barbed geometry with hook-shaped streams (Fig. 3 of Repository 1). Fault and Pisangan-Vadnagar minor lineament (Kumar and Pandit, 2020) control the tectonic activity of the watershed 2 (Fig. 1a). The first-order streams of watershed 3 also show a rectangular pattern of channel arrangement, which seems to be controlled by Mendha stepped fault, neotectonic faults, Jaipur depression and basement faults (Fig. 1a). Towards downstream of the river 3 (watershed 3) a pinnate pattern is found (Fig. 3 of Repository 1). The tributaries originated from the steep sides of inselberg and join the longitudinal master stream at acute angles (Fig. 3 of Repository 1).

### Longitudinal Profile Analysis

Due to rivers' reactivity to tectonic shifts, longitudinal profiles reflect region's tectonic events. Each watershed's main stream was studied for longitudinal profiles. The lengths of the master streams for watersheds 1, 2 and 3 are ~ 285, ~ 169 and ~ 309 km, respectively (Figs. 4a-c). In watershed 2, when the river gradient changes in the midst of the sixth and seventh segments of the long profile, a concave profile is exhibited in the upper reaches. A convex profile and presence of fault/lineament crossing points indicate possibility of tectonic interference along the channel incision progress (Martins et al., 2017). In watershed 3, the master stream flows through the Sambhar lake, a sag pond formed due to the strike-slip Tonk lineament. This lineament was identified based solely on remote sensing studies (Kajale and Deotare, 1997; Wadhawan et al., 2018).

Segments of the longitudinal profile in watershed 1 have SI values between 1.10 to 1.45 (Table 4a). This indicates the entire river is sinuous (Fig. 4a). The master stream of watershed 2 is also sinuous from source to mouth (Table 4b). Sudden changes in sinuosity from 1.35-1.12 at 80 km from the source indicate rejuvenation that may be controlled by the Pisangan – Vadnagar lineament and the unnamed

**Table 3.** Review on dendrogram and clustering in morphometric studies.

Author	Terrain	Country	Software	Approaches / Conclusions
Biswas et al., (2014)	Supin River basin	India	Not mentioned	The basin was been sub-divided into 27 watersheds. Total 36 parameters on river basin geometry, texture of drainage, drainage network and relief have been selected. Each of these parameters was grouped into five clusters on the principle of common morphometric attributes. The parameters have been correlated amongst themselves for the prioritization of hazard prone zones in the hilly terrain.
Chitsaz and Malekian (2016)	Arangeh watershed	Iran	Not mentioned	13 parameters were selected to rank the watersheds based on the susceptibility to soil erosion. The parameters were selected from four categories- soil, climate, geomorphology and topography. The sub-catchments were categorized using the hierarchical clustering approach.
Fenta et al. (2017)	Agula watershed	Ethiopia	Not mentioned	Few morphometric parameters were derived based on the relief features, drainage texture and network, and the basin geometry. Three clusters were made indicating significant geographic heterogeneity.
Karymbalis et al. (2018)	Alluvial fans and catchments in the north Peloponnese	Greece	Matlab v.12b	On the basis of unsupervised categorization, five categories of alluvial fans were identified. It also indicates the relationships between the morphometric traits. The clusters reflect the mechanism involved in the development of alluvial fans.
Prieto-Amparán et al. (2019)	Conchos river basin, part of the 24th Rio Bravo-Conchos hydrological region	Mexico	SAS© 9.1.3	31 watersheds were identified. These watersheds were categorized and then prioritized as per the multivariate methods e.g., principal component analysis and group analysis. Compound parameter ranking approach was applied.
Sakthivel et al. (2019)	Kalrayan Hills, Tamil Nadu	India	SPSS 21	Multi-criteria analytical techniques and hierarchical clustering were performed for the prioritization of watersheds. The analyses confirmed the observed variation of surface to sub-surface flow.
Mohamed (2020)	Qena-Safaga-Bir Queh, Central Eastern Desert	Egypt	StatSoft, Inc. 1995	17 morphometric parameters were used in multivariate statistics. Two clusters, each of which was further divided into four groups, were utilized in the dendrogram analysis in the R-mode.
Eltahan et al. (2021)	Sinai Peninsula	Egypt	Not mentioned	Factor, cluster and regression analyses were carried out to identify the crucial morphometric parameters. The overall coherence of the data confirmed various hydro-morphologic parameters.
Bajracharya and Jain (2022)	Narmada river basin	India	Not mentioned	This work presents different metrics to produce dissimilarity matrices. Hierarchical clustering is used to categorize the watersheds. The categorization of watersheds into a smaller number of dynamically related groups is made possible by the simultaneous study of watershed width functions and hypsometric curves.
Patel et al. (2022)	Ladakh (Trans-Himalaya)	India	SPSS 23	Several morpho-tectonic indices were used to understand the impact of tectonic imprint on the watersheds. To determine the river character in each physiographic unit, these characteristics of the drainage are contrasted with the various lithologic and geomorphic units. A dendrogram was prepared to group the watersheds based on homogeneity.
Biswas et al. (this work)	Bikaner-Nagaur Basin and surroundings, western Rajasthan	India	SPSS 23	Linear parameters - SL, SI and $\theta$ , were used to decipher the tectonics.

thrust (Fig. 4b). In watershed 3, the river varies between the sinuous and meandering pattern (Table 4c). This variation may be due to the differential uplift rates produced due to the neotectonic faults and lineaments that pass through the region and enhance more incision of the channel (Fig. 4c).

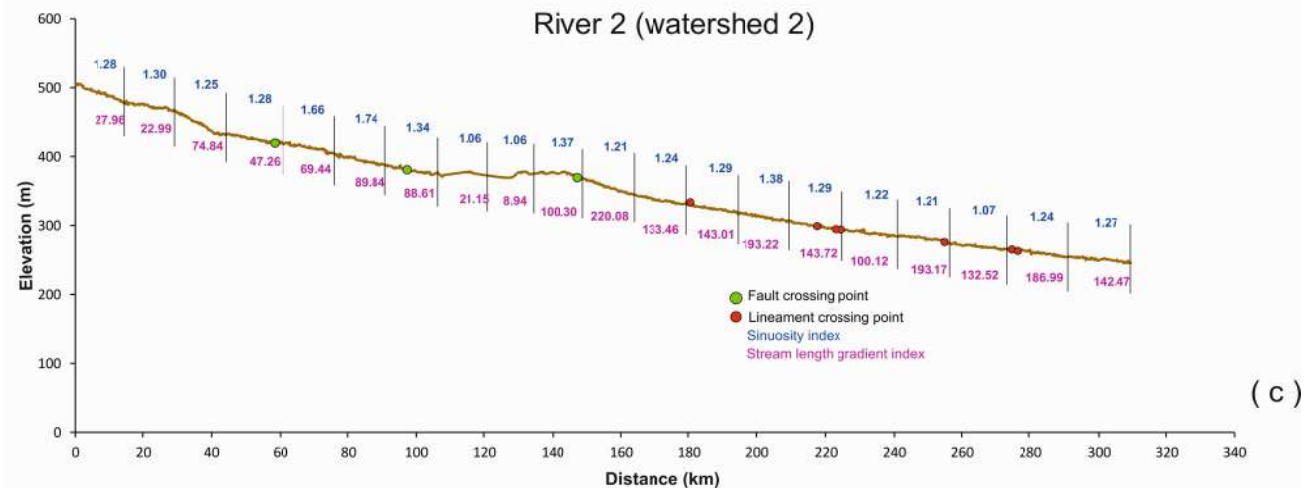
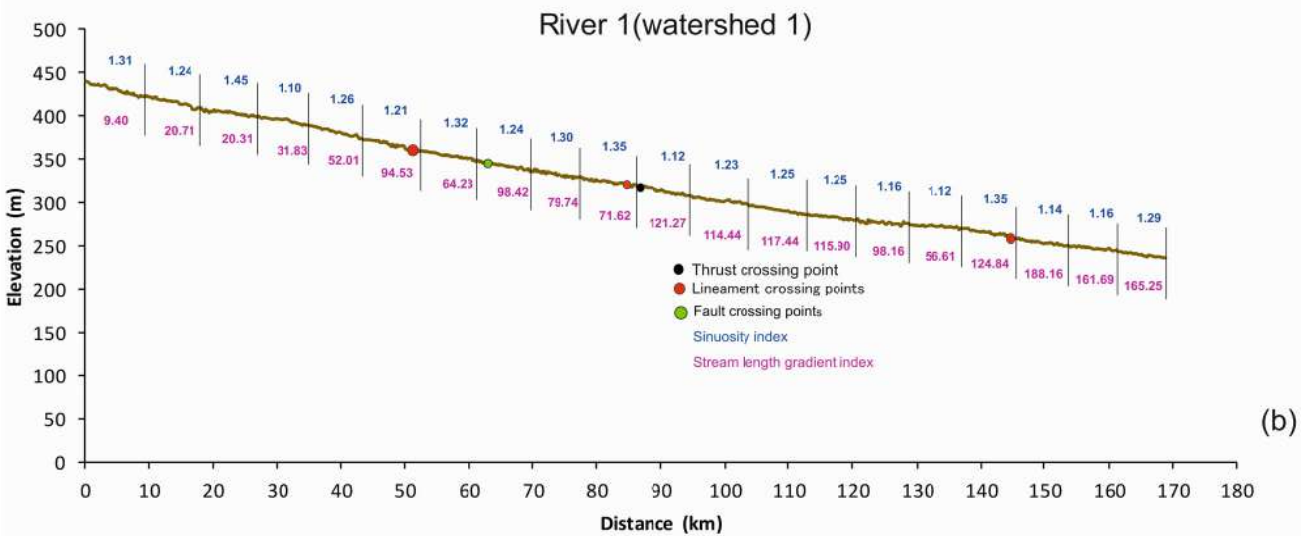
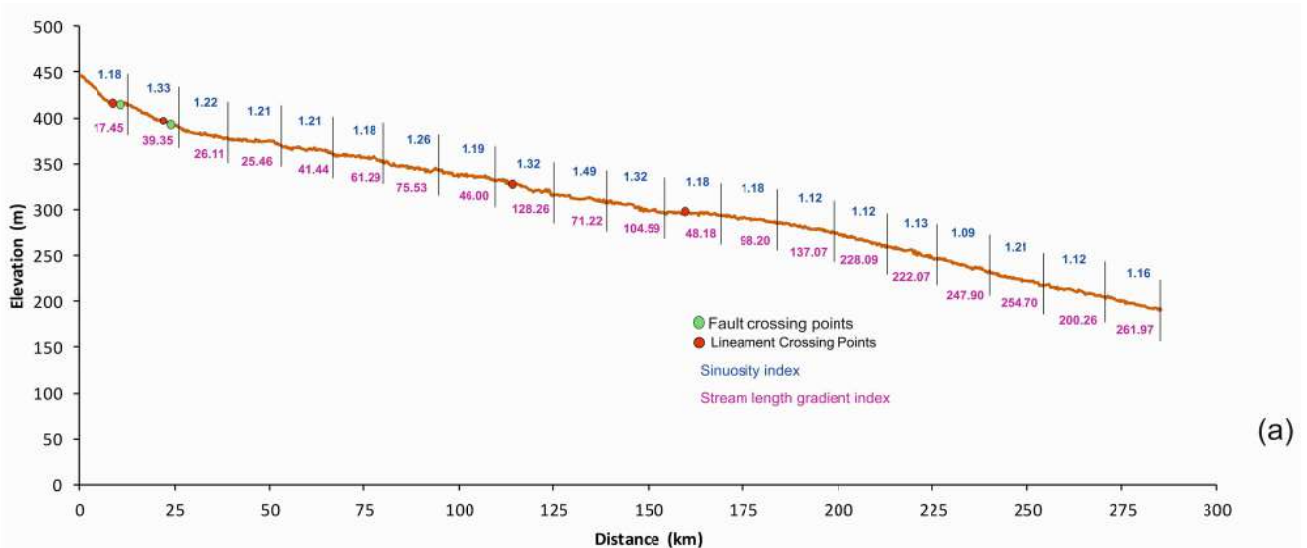
The SL values increase from the source to the mouth of the river in watersheds 1 and 2 except a drop in the segment 9 of watershed 1 (Fig. 4a), and in segments 10 and 11 for watershed 2 (Fig. 4b). In watershed 3, there are several fault/lineament crossing points as in segments 9, 16 and 19. Here the SL values are significant: 8.94 - 100.30, 100.12-197.17 and 132.52 – 186.99, respectively. The eleventh, fourteenth and fifteenth segments (watershed 3) show a maximum increase in the SL values. These elevated magnitudes are 220.08, 193.22 and 193.17, respectively, which may be due to the recent activity of the Tonk lineament. Most of the recent seismic events

are concentrated in watershed 3: In the same watershed, horst/graben fault system developed, and neotectonic faults pass (Fig. 1a).

The master streams of watersheds 1 and 3 exhibit the highest  $R^2$  values in linear curve fitting (0.9891 and 0.9995, respectively). The master streams of watershed 2 exhibits the highest  $R^2 = 0.9982$  in the exponential curve. These three profiles display a linear to exponential model and reduced  $\theta$ . This indicates that the path of the rivers 1 (watershed 1) and 2 (watershed 2) strongly incised vertically in response to recent tectonic events (as in Biswas et al., 2022a,b from Barmer and Jaisalmer basins, respectively). Thus master streams of watershed 1 and 3 are tectonically very active and river 2 is tectonically active as per the best-fit curve model of Lee and Tasi (2009) (Fig.4a-d).

#### Concavity Index ( $\theta$ )

Amongst the considered channels  $\theta$  varies due to the diverse



	Linear R <sup>2</sup>	Exponential R <sup>2</sup>	Logarithmic R <sup>2</sup>	Power curve R <sup>2</sup>
<b>River 1 (watershed 1)</b>	<b>0.9891</b>	<b>0.9744</b>	<b>0.7189</b>	<b>0.6373</b>
<b>River 2 (watershed 2)</b>	<b>0.9891</b>	<b>0.9982</b>	<b>0.7251</b>	<b>0.6801</b>
<b>River 3 (watershed 3)</b>	<b>0.9995</b>	<b>0.9906</b>	<b>0.7696</b>	<b>0.7124</b>

(d)

**Fig. 4 (a) – (c)** Long profiles of rivers 1, 2 and 3 (belonging to the watersheds 1, 2 and 3, respectively). With regard to each segment, SI and SL are estimated at the sites where faults and lineaments intersect. **(d)** Comparative values of R<sup>2</sup> model for linear, exponential, logarithmic and power curve fit.

structural and lithologic control. Amongst the four classes, the results show extremely low  $\theta$  ( $< 4$ ) of rivers 1 from segments 1-13, river 2 from 10 -12, 14, 15, and in river 3 from 1-9. Segment 16 of river 3 indicates a steep channel with bed load sediment. Segments 14 (river 1), 13, 17-19 (river 2), and 10-15, 18 and 20 (river 3) exhibit moderate value (0.41-0.70) that justify the starting of concave nature with less vertical incision. High values (0.71-1.0) are found for segments 15 and 19 (river 1), 20 (river 2) and 17-19 (river 3). Therefore these segments can expand laterally. Finally, there are only two segments; indicating extreme lateral expansion of channel erosion, e.g., segment 20 (river 1) and 16 (river 2) with  $> 1$ . Where the master streams of watersheds 1, 2 and 3 originate. But the concavity values alter towards the downstream of the river course. For instance, in river 2 between segments 12 and 13, increases from 0.377 to 0.475, then decreases again in segment 15 ( $= 0.197$ ), close to the Pisangan - Vadnagar lineament (Figs. 5a,b).

### Hypsometric Curve (HC)

The three parts of HC- head, body and toe- indicate the different stages of profile evolution. The considered master streams in watersheds 1, 2 and 3 are concave up (Akinwumiju, 2021) in 'head' and 'body' sections and a minor portion is concave down. At the points of inflection, the curvature of the HC is minimum. HC values of river 1 is 0.48, river 2 is 0.47 and river 3 is 0.46. These results indicate decreasing slope gradient at the upper reach and an increasing gradient at the lower reach (Akinwumiju, 2021). Minor undulations along the profiles are due to lithologic and structural controls (Akinwumiju, 2021) (Fig. 6).

### Clustering of River Profiles

The prepared dendrogram from the  $d_R$  values enabled clustering of the 60 segments (Fig. 4 of Repository 1) of watersheds 1, 2 and 3 (Fig 4 in Repository 1). Cluster analysis of river profiles can compare

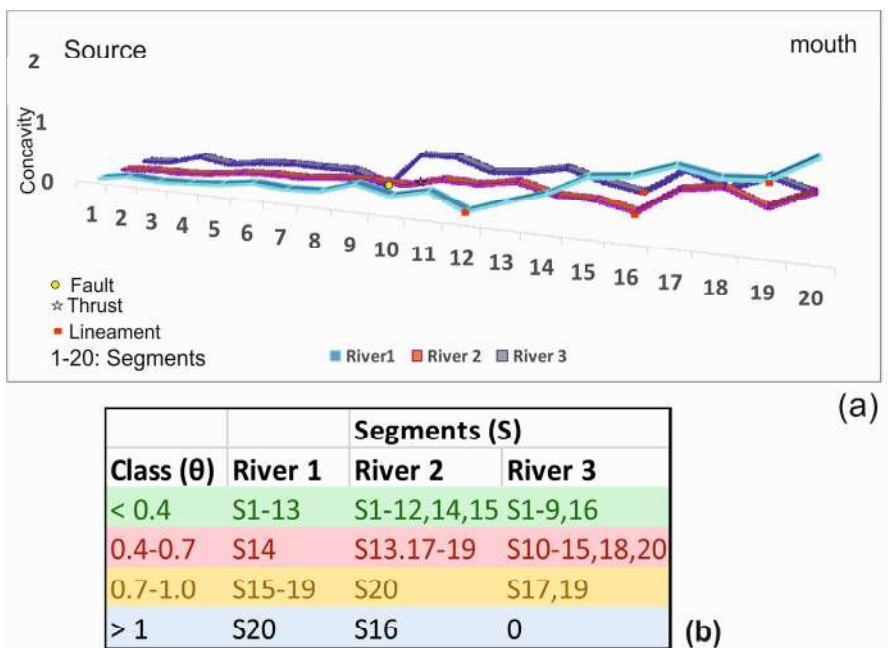


Fig. 5 (a) Graphical representation of  $\theta$  for each marked segment of three respective rivers. Faults and lineaments are marked from source to mouth. (b) Four classes of  $\theta$  for the three rivers are computed.

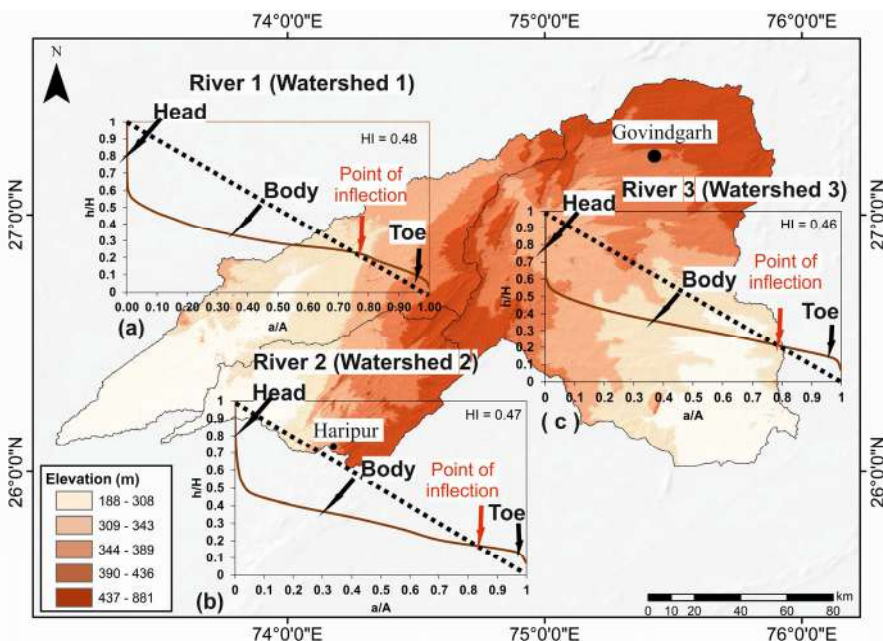


Fig. 6. Using ArcGIS 10.4, the hypsometric curves of three rivers presented inflection points shown.

the groups of similar river profiles within heterogeneous landscapes. The  $d_r$  values are calculated between each pair of segments to form a symmetric proximity matrix (Table 1 of Repository 4). There are three major clusters as per the rescaled distance cluster combination. These are clusters 1 (S 7, 11, 21, 22, 25, 50, 41, 42, 44 and 47), 2 (S 26, 28, 34, 36, 43, 49, 52, 54, 55, 56, 60) and 3 (S 24, 31, 32, 36, 39, 43, 48, 51, 52, 55, 49, 56, 60). In these clusters, the morphometric indicators SI, SL and  $\theta$  are mutually combined that signify structural control in channel morphology (Bhatt et al., 2020) (Fig. 7).

## DISCUSSIONS

The spatial drainage patterns connote the structural signatures. In the south-eastern part of the basin, basement faults, neotectonic faults and major and minor lineaments control the channels' flow towards south-east and south-west and over the exposed Kumbhalgarh Group, Marh Formation, Mangalwar Group and Bilara Group. Hills at south-west and east are dissected by several channels. Elevated topography related to the unnamed basement faults and lineaments acted as a water divide of three watersheds. Hence, the streams at the south-western part of BNB align sub-parallel to each other.

Development of rectangular, pinnate and complex barbed pattern signify fault lines over which the channels are oriented in watersheds 2 and 3. The linear-scale concavity analysis discloses the effects of existing major faults, thrust and lineaments along the master streams (Fig. 6a) of each watershed where SL values increase downstream and channels are sinuous. Lower  $\theta$  value ( $< 0.4$ ) has resulted from all the channel segments with convex shape of profile prone to more vertical erosion. Near the river's source for watersheds 1 and 3,  $\theta$  is highest, and it decreases towards the mouth of the river. In watershed 2,  $\theta$  is highest at the source, but then it varies between low and high values from the source to the mouth of the river. Low concavities are found in areas where the rock uplift rate increases downstream, while high concavities include the area where rock uplift decreases towards downstream (Kirby and Whipple, 2001). Hence, lower concavities indicate that watersheds 1-3 have high rates of uplift downstream.

60 segments of three watersheds were considered in the dendrogram and the segments of the clusters indicate the similar trend of the SL, SI and  $\theta$  values. These indicate active tectonics in the

**Table 4a.** Linear parameters for determining the dendrogram for the river 1.

River 1					
Segments	latitude (degree)	longitude (degree)	Concavity (unitless)	SI (unitless)	SL (unitless)
	27.25729	75.0247	0	0	0
1	27.19021	74.92957	0.012	1.17	3.651
2	27.18215	74.82124	0.093	1.32	37.80
3	27.17993	74.70402	0.066	1.21	25.77
4	27.12799	74.59958	0.094	1.20	25.28
5	27.07327	74.49848	0.134	1.21	41.26
6	27.00549	74.40376	0.213	1.19	61.12
7	26.95688	74.3021	0.174	1.25	75.38
8	26.87911	74.2196	0.2	1.18	45.92
9	26.82967	74.12405	0.372	1.32	128.12
10	26.79939	74.03322	0.246	1.48	71.15
11	26.70495	73.99044	0.374	1.32	104.51
12	26.61273	73.92739	0.129	1.18	48.150
13	26.56496	73.82045	0.33	1.17	98.151
14	26.50163	73.71407	0.515	1.11	137.00
15	26.42996	73.61546	0.817	1.11	228.00
16	26.37108	73.50436	0.878	1.13	221.98
17	26.2933	73.40991	1.08	1.08	247.82
18	26.22386	73.32131	0.968	1.20	254.63
19	26.16498	73.21603	1.004	1.12	200.21
20	26.11224	73.10219	1.353	1.15	261.91

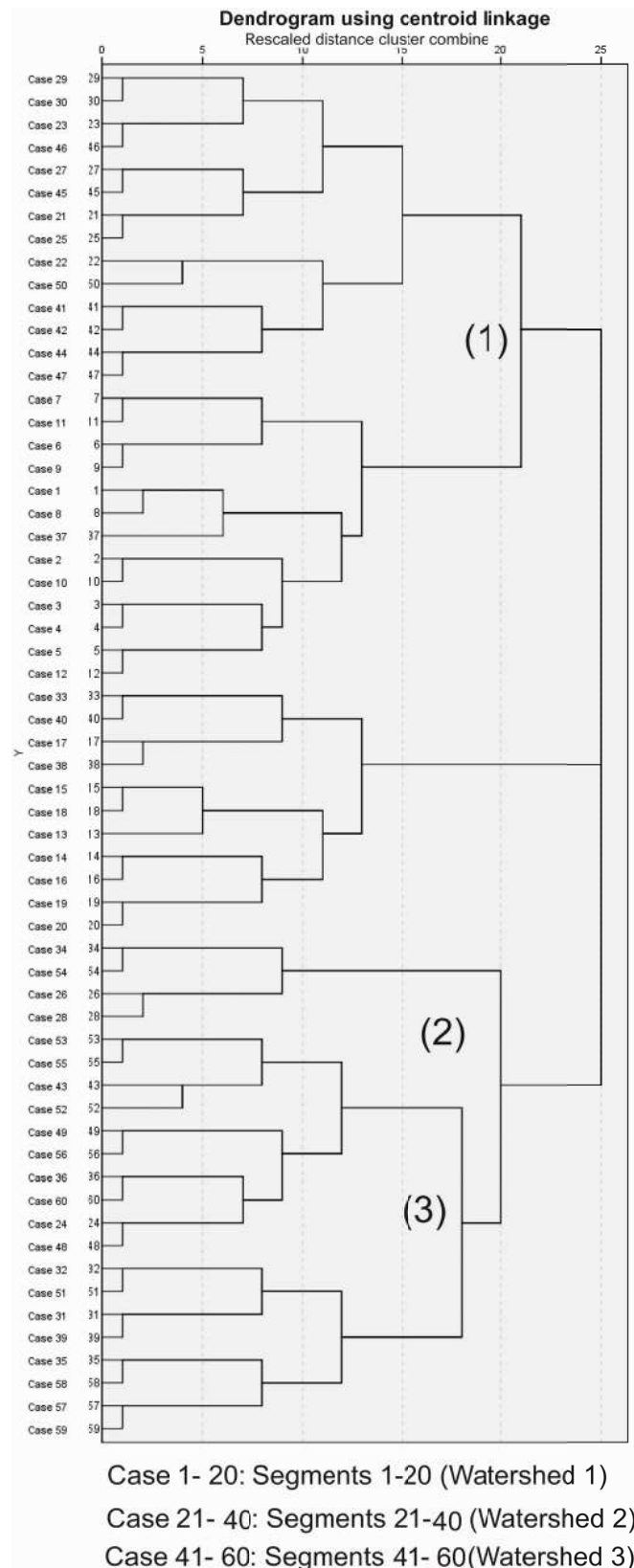


**Fig. 7.** Dendrogram generated with SPSS software utilising centroid linkage with SL, SI, and concavity. Three cluster zones are markers.

considered three watersheds. In micro-scale study, channels of watershed 1 are strongly controlled by lineaments (Fig. 8a). The channel flow (CF) of watershed 2 in the upper part is along the fault. A pinnate drainage pattern in the middle course has developed (Fig. 8a). In watershed 3, neotectonic faults play a dominant role in

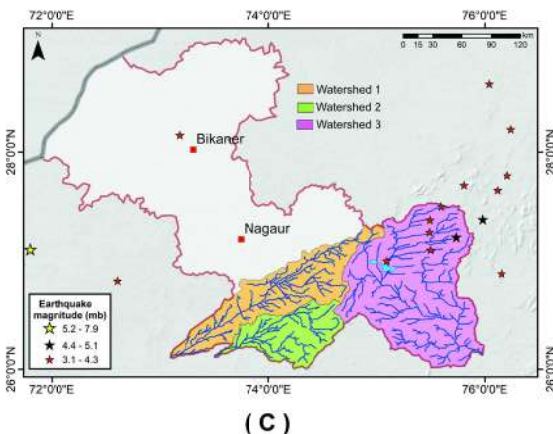
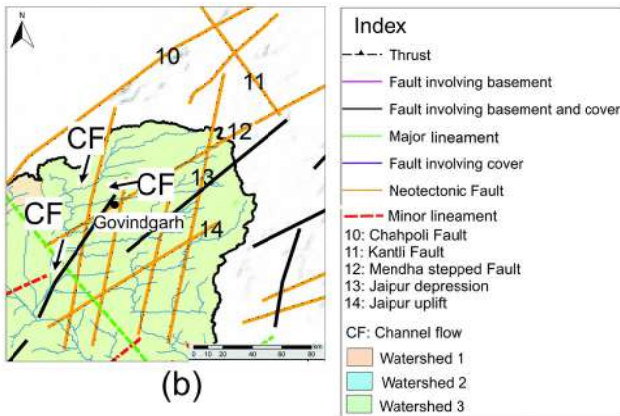
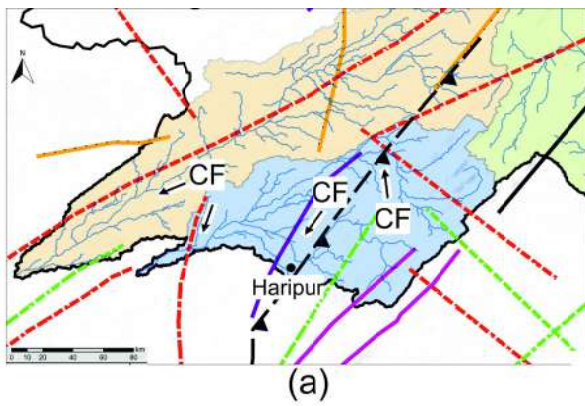


**Fig. 8** (a) Micro-scale study of drainage lines of watersheds 1 and 2 controlled by lineaments/faults. (b) Micro-scale study of drainage lines of watershed 3 controlled by lineaments/faults forming horst/graben (Jaipur depression and Jaipur uplift).

determining CF line and all the first-order streams join by right angle resulting in a rectangular drainage pattern (Fig. 8b). The clusters are associated with morphotectonic linear parameters (SL, SI and  $\theta$ ). The distribution of low (3.1-4.3 mb) to moderate (4.4-5.1 mb) magnitude earthquakes over watershed 3 justifies its tectonic activity (Fig. 8c).

Morphometric analyses of the considered two spots also confirm the tectonic intervention in channel incision resulting in straight flow path of small gullies and inception of rectangular to sub-parallel drainage pattern. The micro-scale study justifies the tectonic control on rivers.

Regional geomorphic study of BNB explains the importance of neotectonics. Aeolian geomorphic evolution produced landforms that were reshaped by channel aggradation/degradation. There are nine prominent units in the three watersheds, 1, 2 and 3- aeolian plains, highly dissected hills and valleys, moderately dissected hills and

**Table 4b.** Linear parameters for determining the dendrogram for the river 2

River 2					
Segments	latitude (degree)	longitude (degree)	Concavity (unitless)	SI (unitless)	SL (unitless)
	26.2608	74.53973	0	0	0
1	26.27747	74.48181	0.004	1.31	9.40
2	26.33247	74.45487	0.047	1.24	20.71
3	26.35108	74.39681	0.048	1.45	20.30
4	26.4158	74.38237	0.082	1.10	31.83
5	26.47718	74.37376	0.162	1.26	52.01
6	26.52718	74.32932	0.194	1.20	94.52
7	26.51885	74.26627	0.193	1.32	64.22
8	26.50274	74.20155	0.251	1.24	98.42
9	26.48191	74.1446	0.275	1.30	79.73
10	26.4408	74.09461	0.253	1.35	71.62
11	26.40913	74.02933	0.392	1.11	121.26
12	26.3658	73.98072	0.377	1.22	114.97
13	26.34136	73.91656	0.475	1.25	117.43
14	26.30136	73.86739	0.328	1.24	115.89
15	26.27886	73.80073	0.32	1.16	98.15
16	26.23331	73.74629	0.197	1.12	56.60
17	26.20386	73.69129	0.599	1.34	124.83
18	26.19136	73.61741	0.69	1.13	188.15
19	26.15164	73.56296	0.454	1.15	161.69
20	26.11206	73.50991	0.74	1.29	165.25

**Table 4c.** Linear parameters for determining the dendrogram for the river 3

River 3					
Segments	latitude (degree)	longitude (degree)	Concavity (unitless)	SI (unitless)	SL (unitless)
	27.48908	75.67092	0	0	0
1	27.48047	75.54621	0.008	1.27	27.96
2	27.43325	75.43538	0.042	1.29	22.98
3	27.38075	75.32705	0.192	1.25	74.83
4	27.28548	75.26705	0.107	1.28	47.25
5	27.23521	75.19067	0.183	1.65	69.43
6	27.15549	75.18622	0.224	1.73	89.83
7	27.05882	75.16067	0.216	1.33	88.61
8	26.89883	75.11012	0.222	1.06	21.15
9	26.80911	75.04734	0.029	1.06	8.93
10	26.76773	75.14039	0.588	1.36	100.29
11	26.67412	75.21039	0.604	1.21	220.08
12	26.58746	75.28566	0.415	1.24	133.46
13	26.54718	75.39344	0.467	1.29	143.01
14	26.48246	75.4901	0.582	1.38	193.22
15	26.47524	75.60426	0.431	1.29	143.72
16	26.46218	75.73175	0.326	1.22	100.11
17	26.34608	75.72981	0.718	1.21	193.17
18	26.22636	75.75203	0.499	1.06	132.51
19	26.18997	75.86786	0.732	1.24	186.99
20	26.13137	75.97258	0.557	1.27	142.46

valleys, pediment-pediain complex, pediment slope, active flood plain, alluvial plain, highly dissected hills and valleys; and moderately dissected hills and valleys (Fig. 9a). Highly and moderately dissected hills/valleys are mostly structure-controlled. After the exogenetic erosional activities by both wind and rivers, these geomorphic features survived as hillocks and inselbergs/residuals. The micro-scale spot analysis (Fig. 9b) clearly depicts the geomorphic units where the channels are controlled by faults and lineaments. Besides, the horst/graben structures in watershed 3 developed what were named by previous authors (Mondal et al., 2022) as the Jaipur depression and the Jaipur uplift. These locations have been seismically active in the last 100 years.

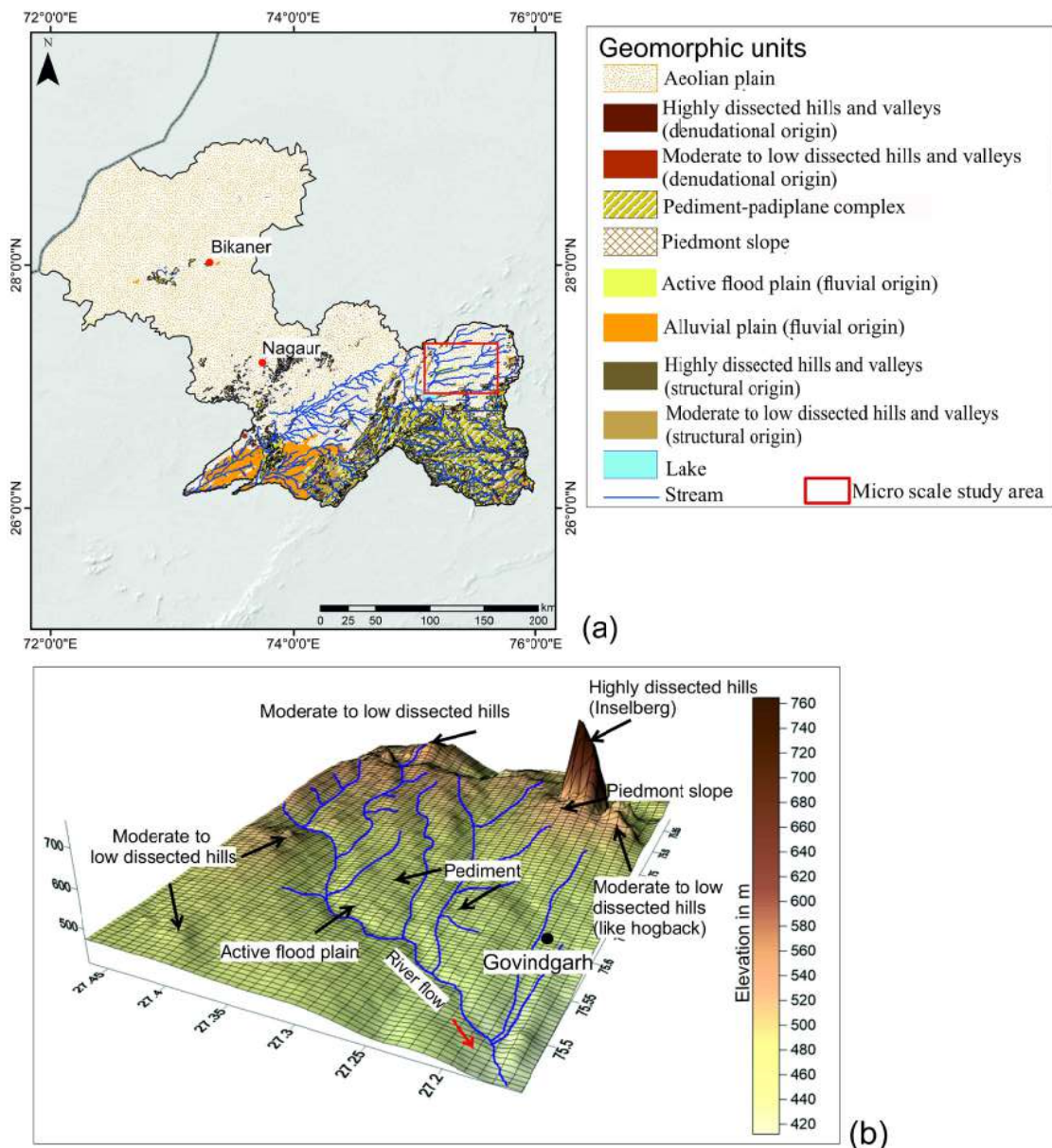


**Fig. 9** (a) Map showing the nine geomorphic units and identified landforms in BNB (<https://bhukosh.gsi.gov.in/Bhukosh/Public> (Accessed on 09-Feb-2023)). Aeolian cycle developed pediments and active flood plains. (b) Geomorphic units containing parallel slope retreat remains such as dissected hills and Inselberg created by aeolian erosion were identified through micro-scale studies.

## CONCLUSIONS

The study establishes links between a few of the BNB's outcrops and sub-surface features/structures using morphotectonics. The main results are:

- The frequent variation in the values of along the reaches of the three considered mainstreams imply tectonic imprint. The best-fit models show highest  $R^2$  in linear model for watersheds 1 and 3. This indicates that the channels are quite sensitive tectonically. The profile of river 2 in watershed 2 shows highest  $R^2$  of exponential best-fit curve. This refers to a high tectonic activity as well.
- The three identified clusters of river profiles in the three watersheds enable easy comparison of the river segments with interlinked values of SL, SI and  $\theta$ .
- Amongst all three watersheds, watershed 3 is mostly influenced by active tectonics. Faults, lineaments, horst/graben structures and recent earthquakes justify the tectonic sensitivity of the area. The south-eastern section of BNB including watershed 3 is a part of the Aravalli-Delhi Fold Belt. This work therefore questions

the conventional idea that considers Aravalli to be a tectonically stable region.

- Watershed 3 appears to be tectonically active with the presence of several structures. A thorough research may be conducted utilising the Ground Penetrating Radar (GPR) and seismic studies to check whether any structural traps exist there.

*Acknowledgements:* This work was initiated during the seed project (grant number RD/0120-PSUCE19-001) received from the Center of Excellence in Oil, Gas and Energy, IIT Bombay. We thank the Chief Editor Prof. G.M. Bhat (University of Jammu), the Handling Editor Prof. Pradeep Srivastava (IIT Roorkee) and the anonymous reviewers for providing critical comments that improved the work.

## References

- Agar, R.A. (1987) The Najd fault system revisited; a two-way strike-slip orogen in the Saudi Arabian Shield. *Jour. Struct. Geol.*, v.9, pp.41-48, [https://doi.org/10.1016/0191-8141\(87\)90042-3](https://doi.org/10.1016/0191-8141(87)90042-3).
- Aiken, S.J. and Brierley, G.J. (2013) Analysis of longitudinal profiles along

- the eastern margin of the Qinghai-Tibetan Plateau, *Jour. Mountain Sci.*, v.10(4), pp.643–657, <https://doi.org/10.1007/s11629-013-2814-2>.
- Al-Husseini, M.I. (2000) Origin of the Arabian Plate structures: Amar collision and Najd rift. *Geo Arabia*, v.5(4), pp.527-542.
- Ambili, V. and Narayana, A.C. (2014) Tectonic effects on the longitudinal profiles of the Chaliyar River and its tributaries, Southwest India, *Geomorph.*, v.217, pp.37–47, <https://doi.org/10.1016/j.geomorph.2014.04.013>.
- Anand, A.K. and Pradhan, S.P. (2019) Assessment of active tectonics from geomorphic indices and morphometric parameters in part of Ganga basin. *Jour. Mountain Sci.*, v.16(8), pp.1943–1961. <https://doi.org/10.1007/s11629-018-5172-2>.
- Akinwumiju, A. S. (2021) Characterization of Hypsometric Curves using ArcGIS and R. Programming Language. *IFE Res. Publ. Geography*, v.19(1), pp.86-101 <https://irpg.oauife.edu.ng/index.php/irpg.2021>.
- Bakliwal, P.C. and Ramasamy, S.M. (1987) Lineament Fabric of Rajasthan and Gujarat, India. *Rec. Geol. Surv. India*, v.113(7), pp.54-64.
- Bajracharya, P. and Jain, S. (2022) Hydrologic similarity based on width function and hypsometry: An unsupervised learning approach. *Computers and Geosciences*, v.163, 105097, <https://doi.org/10.1016/j.cageo.2022.105097>.
- Bhatt, S.C., Singh, R., Ansari, M.A. and Bhatt, S. (2020) Quantitative Morphometric and Morphotectonic Analysis of Pahuj Catchment Basin, Central India. *Jour. Geol. Soc. India*, v.96(5), pp.513-520. <https://doi.org/10.1007/s12594-020-1590-1>.
- Bhattarai, I. (2017) Quantitative River Profile Analysis to Investigate Exhumation of the Siwalik Foreland Basin, Nepalese Himalaya. Masters Theses & Specialist Projects. Paper 1932. <http://digitalcommons.wku.edu/theses/1932>.
- Bhola, A.M., Sharma, B.K. and Ghosh, S.K. (2004) Folds in multilayered rocks of Proterozoic age, Rajasthan, India. *Jour. Earth Syst. Sci.*, v.113, pp.299-311.
- Biswas, A., Das Majumdar, D. and Banerjee, S. (2014) Morphometry governs the dynamics of a drainage basin: Analysis and implications. *Geography Jour.*, pp.1–14, <https://doi.org/10.1155/2014/927176>.
- Biswas, M., Gogoi, M.P., Mondal, B., Sivasankar, T., Mukherjee, S. and Dasgupta, S. (2022a) Geomorphic assessment of active tectonics in Jaisalmer basin (western Rajasthan, India). *Geocarto Internat.* <https://doi.org/10.1080/10106049.2022.2066726>.
- Biswas, M., Puniya, M.K., Gogoi, M.P., Dasgupta, S., Mukherjee, S. and Kar, N.R. (2022b) Morphotectonic analysis of petroliferous Barmer rift basin (Rajasthan, India). *Jour. Earth Syst. Sci.*, v.131, pp.5-6.
- Bhowmick, P.K. (2008) Phanerozoic petroliferous basin of India. *Glimpses of Geosci. Res. India*, pp.253–268.
- Bhatt, S.C., Singh, R., Ansari, M.A. and Bhatt, S. (2020) Quantitative morphometric and morphotectonic analysis of Pahuj Catchment Basin, Central India, *Jour. Geol. Soc. India*, v.96(5), pp.513–520. <https://doi.org/10.1007/s12594-020-1590-1>.
- Bragança, M.T., Barros, L.F. and Oliveira, D. de (2021) Using morphometric and geomorphic indices to assess western São Francisco Craton neotectonic traces. *Geography Department University of Sao Paulo*, v.41, <https://doi.org/10.11606/eissn.2236-2878.rdg.2021.184588>.
- Chitsaz, N. and Malekian, A. (2016) Development of a risk-based multi-criteria approach for watershed prioritization with consideration of soil erosion alleviation (Case study of Iran). *Environ. Earth Sci.*, v.75(22), <https://doi.org/10.1007/s12665-016-6256-3>.
- Chen, C.Y. and Willett, S.D. (2016) Graphical methods of river profile analysis to unravel drainage area change, uplift and erodibility contrasts in the Central Range of Taiwan. *Earth Surf. Process Landf.*, v.41(15), pp.2223–2238.
- Clubb, F.J., Bookhagen, B. and Rheinwalt, A. (2019) Clustering river profiles to classify geomorphic domains. *Jour. Geophys. Res. Earth Surf.*, v.124(6), pp.1417-1439.
- Cyr, A.J., Granger, D.E., Olivetti, V. and Molin, P. (2014) Distinguishing between tectonic and lithologic controls on bedrock channel longitudinal profiles using cosmogenic <sup>10</sup>Be erosion rates and channel steepness index. *Geomorph.*, v.209, pp.27-38.
- Das, A.R. (1988) Geometry of the superposed deformation in the Delhi Supergroup of rocks, north of Jaipur, Rajasthan. In: A.B. Roy (ed), Precambrian of the Aravalli Mountain, Rajasthan, India. *Jour. Geol. Soc. India*, v.7, pp.247-266.
- Duvall, A., Kirby, E. and Burbank, D. (2004) Tectonic and lithologic controls on bedrock channel profiles and processes in coastal California. *Jour. Geophys. Res. Earth. Surf.*, v.109(F3), pp.118.
- Eltahan, A.M., Abd Elhamid, A.M. and Abdelaziz, S.M. (2021) Multivariate statistical analysis of geomorphological parameters for Sinai Peninsula, *Alexandria Eng. Jour.*, v.60(1), pp.1389–1402, <https://doi.org/10.1016/j.aej.2020.10.059>.
- Farooq, U., Chetia, R., Mathews, R., Srivastav, S., Singh, B. and Singh, V. (2019) Palaeodepositional conditions and hydrocarbon source characteristics of lignites from Bikaner-Nagaur Basin (Rajasthan) western India based on organic petrographic studies. In: Naj Aziz and Bob Kininmonth (Eds.), Proceedings of the 2019 Coal operators conference, Mining Engineering, University of Wollongong, v.18-20, pp.352-367.
- Fenta, A.A., Yasuda, H., Shimizu, K., Haregeweyn, N. and Woldearegay, K. (2017) Quantitative analysis and implications of drainage morphometry of the Agula watershed in the semi-arid northern Ethiopia, *Appl. Water Sci.*, v.7(7), pp. 3825–3840. <https://doi.org/10.1007/s13201-017-0534-4>.
- Hack, J.T. (1957) Studies of longitudinal stream profiles in Virginia and Maryland. USGS Prof. Paper, <https://doi.org/10.3133/pp294b>.
- Hack, J.T. (1973) Stream-profile analysis and stream-gradient index. *Jour. Res. US Geol. Surv.*, v.1(4), pp.421-429.
- Han, Z., Li, X., Wang, N., Chen, G., Wang, X. and Lu, H. (2017) Application of river longitudinal profile morphometrics to reveal the uplift of Lushan Mountain. *Acta Geol. Sin English Edition*, v.91(5), pp.1644-1652.
- Gandhi, D., Prajapati, P., Prizomwala, S. P., Bhatt, N. and Rastogi, B. K. (2015) Delineating the spatial variability in neotectonic activity along the southwestern Saurashtra, Western India, *Zeits. für Geomorph.*, v.59(1), pp.21–36, <https://doi.org/10.1127/0372-8854/2014/0122>.
- George, B.G. (2019) Geology of the Neoproterozoic – early Cambrian Marwar Supergroup, Rajasthan: A synthesis, *Proc. Indian Nat. Sci. Acad.*, <https://doi.org/10.16943/ptinsa/2019/49712>.
- Kajale, M.D. and Deotare, B.C. (1997) Late Quaternary environmental studies on salt lakes in western Rajasthan, India: a summarised view. *Jour. Quaternary Sci.*, v.12(5), pp.405-412.
- Keller, E.A. and Pinter, N. (1996) Active tectonics (Vol. 338). Upper Saddle River, NJ: Prentice Hall.
- Keller, E. and Pinter, N. (2002) Active Tectonics Earthquakes, Uplift and Landscape. 2nd ed. Upper Saddle River, New Jersey: Prentice Hall.
- Karymbalis, E., Ferentinou, M. and Giles, P.T. (2016) Use of morphometric variables and self-organizing maps to identify clusters of alluvial fans and catchments in the North Peloponnese, Greece. In: Ventra, D. and Clarke, L.E. (Eds.), *Geol. Soc., London, Spec. Publ.*, v.440, pp.45–64, doi:10.1144/sp440.7.
- Kale, V.S., Sengupta, S., Achyuthan, H. and Jaiswal, M.K. (2014) Tectonic controls upon Kaveri River drainage, cratonic peninsular India: Inferences from longitudinal profiles, morphotectonic indices, hanging valleys and fluvial records, *Geomorphology*, v.227, pp.153–165, <https://doi.org/10.1016/j.geomorph.2013.07.027>.
- Kothiyari, G.C. and Rastogi, B.K. (201) Tectonic control on drainage network evolution in the upper Narmada Valley: Implication to neotectonics. *Geography Jour.*, v.3, pp.1–9. <https://doi.org/10.1155/2013/325808>, 2013.
- Kothiyari, G.C., Singh, A.P., Mishra, S., Kandregula, R.S., Chaudhary, I. and Chauhan, G. (2018) Evolution of drainage in response to brittle - ductile dynamics and surface processes in Kachchh Rift Basin, Western India, *Tectonics - Problems of Regional Settings*. <https://doi.org/10.5772/intechopen.73653>.
- Kirby, E. and Whipple, K. (2001) Quantifying differential rock-uplift rates via stream profile analysis. *Geology*, v.29(5), pp.415-418.
- Kirby, E. and Whipple, K.X. (2012) Expression of active tectonics in erosional landscapes. *Jour. Struct. Geol.*, v.44, pp.54-75.
- Kumar, H. and Pandit, M. (2020) Recurrent seismicity in Rajasthan State in the tectonically stable NW Indian Craton. *Iranian Jour. Earth Sci.*, v.12(1), pp.1-9.
- Kumar, V., Chandra, R. and Rastogi, S. (2005) Geology and evolution of Nagaur-Ganganagar Basin with special reference to salt and potash mineralization. *Geol. Surv. India Spec. Publ.*, v.62, pp.1-151.
- Lee, C. and Tsai, L. (2009) A quantitative analysis for geomorphic indices of longitudinal river profile: a case study of the Choushui River, Central Taiwan. *Environ. Earth Sci*, v.59(7), pp.1549-1558.
- Leopold, L., Wolman, M. and Miller, J. (1964) Fluvial processes in geomorphology. San Francisco: W.H. Freeman.
- Lu ning, S., craig, J., loydell, D. K., Sjtorch, P. & Fitches, W. R. (2000) Lowermost Silurian 'hotshales' in North Africa and Arabia: regional distribution and depositional model. *Earth Sci. Rev.*, v.49, pp.121–200.
- Mandal, A., Saha, D. and Kumar, A. (2021) Structural analysis and seismic stratigraphy for delineation of Neoproterozoic-Cambrian petroleum system in central and eastern part of Bikaner–Nagaur basin, India. *Jour. Pet. Explor. Prod. Tech.*, pp.1-17.
- Marple, R.T. and Talwani, P. (2000) Evidence for a buried fault system in the

- Coastal Plain of the Carolinas and Virginia—implications for neotectonics in the southeaster United States. *Geol. Soc. Amer. Bull.*, v.112(2), pp.200-220.
- Martins, A.A., Cabral, J., Cunha, P.P., Stokes, M., Borges, J., Caldeira, B. and Martins, A.C. (2017) Tectonic and lithological controls on fluvial landscape development in central-eastern Portugal: Insights from long profile tributary stream analyses. *Geomorphology*, v.276, pp.144-163. .
- Mathews, R.P., Chetia, R., Agrawal, S., Singh, B.D., Singh, P. K., Singh, V.P. and Singh, A. (2020) Early Palaeogene climate variability based on n-alkane and stable carbon isotopic composition evidenced from the Barsingsar Lignite-bearing sequence of Rajasthan. *Jour. Geol. Soc. India*, v.95(3), pp.255-262.
- Mohamed, E.K. (2020) Watershed delineation and morphometric analysis using remote sensing and GIS mapping techniques in Qena-Safaga-Bir Queh, Central Eastern Desert. *Internat. Jour. Water Resour. Environ. Eng.*, v.12(2), pp.22-46., <https://doi.org/10.5897/ijwree2019.0896>.
- Patel, P.P., Guha, S., Das, D. and Bose, M. (2022) Spatial variability of topographic attributes and channel morphological characteristics in the ladakh trans-himalayas and their tectonic and structural controls. *Himalayan Neotectonics and Channel Evolution*, pp.67-110, [https://doi.org/10.1007/978-3-030-95435-2\\_3](https://doi.org/10.1007/978-3-030-95435-2_3), 2022.
- Pollastro, R.M. (1999) Ghaba Salt Basin Province and Fahud Salt Basin Province, Oman: *Jour. Pet. Geol.*, (25). US Department of the Interior, USGS.
- Prasad, B., Asher, R. and Borgohai, B. (2010) Late Neoproterozoic (Ediacaran)-Early Paleozoic (Cambrian) Acritarchs from the Marwar Supergroup, Bikaner-Nagaur Basin, Rajasthan. *Jour. Geol. Soc. India*, v.75(2), pp.415-431.
- Prieto-Amparán J.A., Pinedo-Alvarez A., Vázquez-Quintero G., Valles-Aragón M.C., Rascón-Ramos A.E., Martínez-Salvador M, and Villarreal-Guerrero F. (2019) A multivariate geomorphometric approach to prioritize erosion-prone watersheds. *Sustainability*, v.11(18), 5140, <https://doi.org/10.3390/su11185140>.
- Pérez-Peña, J.V., Azañón, J.M. and Azor, A. (2009) CalHypso: AnArcGIS extension to calculate hypsometric curves and their statistical moments. Applications to drainage basin analysis in SE Spain. *Comput Geosci*, v.35, 1214-1223.
- Prakash, K., Mohanty, T., Pati, J. K., Singh, S. and Chaubey, K. (2016) Morphotectonics of the Jamini River Basin, Bundelkhand craton, Central India; using remote sensing and GIS technique. *Appl. Water Sci.*, v.7(7), pp.3767-3782. <https://doi.org/10.1007/s13201-016-0524-y>.
- Raju, S.V., Mathur, N. and Sarmah, M.K. (2014) Geochemical characterization of Neoproterozoic heavy oil from Rajasthan, India: implications for future exploration of hydrocarbons. *Curr. Sci.*, pp.1298-1305.
- Ram, J. (2015) Neoproterozoic successions in Peninsular India and their hydrocarbon prospectively. In: Bhat, G.M., Craig, J., Thurow, J. W., Thusu, B. & Cozzi, A. (Eds.), *Geology and Hydrocarbon Potential of Neoproterozoic-Cambrian Basins in Asia*. *Geol. Soc. London, Spec. Publ.*, v.366, pp.59-73.
- Rajak, P.K., Singh, V.K., Singh, P.K., Singh, M.P. and Singh, A.K. (2019) Environment of paleomire of lignite seams of Bikaner-Nagaur basin, Rajasthan (W. India): petrological implications. *Internat. Jour. Oil Gas Coal Tech.*, v.22(2), pp.218-245.
- Rasheed, M.A., Lakshmi, M., Srinu, D. and Dayal, A.M. (2011) Bacteria as indicators for finding oil and gas reservoirs: A case study of the Bikaner-Nagaur Basin, Rajasthan, India. *Pet. Sci.*, v.8(3), pp.264-268.
- Roy, A.B. (2006) Seismicity in the Peninsular Indian Shield: some geological considerations. *Curr. Sci.*, pp.456-463, .
- Sakthivel, R., Jawahar Raj, N., Sivasankar, V., Akhila, P. and Omine, K. (2019) Geo-spatial technique-based approach on drainage morphometric analysis at Kalrayan Hills, Tamil Nadu, India, *Appl. Water Sci.*, v.9(1), <https://doi.org/10.1007/s13201-019-0899-7>.
- Seeber, L. and Gornitz, V. (1983) River profiles along the Himalayan arc as indicators of active tectonics. *Tectonophysics*, v.92(4), pp.335-367.
- Siahaan, M. R., Sukiyah, E., Sulaksana, N. and Harwat Haryanto, A.D. (2022) Assessment of Active Tectonic from Morphometric Properties in Krueang Raya Watershed, Aceh Besar, Indonesia. *Eng. Lett.*, v.30(3), EL-3--3-20.
- Singh, A., Shivanna, M., Mathews, R.P., Singh, B.D., Singh, H., Singh, V.P. and Dutta, S. (2017) Paleoenvironment of Eocene lignite bearing succession from Bikaner-Nagaur Basin western India: Organic petrography, palynology, palynofacies and geochemistry. *Int. Jour. Coal Geol.*, v.181, pp.87-102.
- Singh, A.K., Hakimi, M.H., Kumar, A., Ahmed, A., Abidin, N.S.Z., Kinawy, M., Mahdy, O.E. and Lashin, A. (2020) Geochemical and organic petrographic characteristics of high bituminous shales from Gurha mine in Rajasthan, NW India. *Sci. Rep.*, v.10(1), pp.1-19.
- Sinha, R. and Raymahashay, B.C. (2004) Evaporite mineralogy and geochemical evolution of the Sambhar Salt Lake, Rajasthan, India. *Sediment. Geol.*, v.166(1-2), pp.59-71.
- Solanki, T., Solanki, P. M., Makwana, N., Prizomwala, S. and Kothiyari, G. C. (2021) Geomorphologic response to neotectonic instability in the Deccan Volcanic Province, Shetrunji River, Western India: Insights from Quantitative Geomorphology. *Quaternary Internat.*, v.575-576, pp.96-110, <https://doi.org/10.1016/j.quaint.2020.06.015>.
- Stepančikova, P., Stemberk, J. and Vilimek, V. (2008) Neotectonic movements in the East Sudeten Mountains and monitoring of recent fault displacements (Czech Republic). *Geomorphology*, v.102, pp.68-80.
- Strahler, A.N. (1952) Hypsometric (area-altitude) analysis of erosional topography. *Geol. Soc. Amer. Bull.*, v.63(11), pp.1117-1142.
- Whipple, K. (2004) Bedrock rivers and the geomorphology of active orogens. *Ann. Rev. Earth Planet. Sci.*, v.32, pp.151-185.
- Whittaker, A.C., Cowie, P.A., Attal, M., Tucker, G.E. and Roberts, G.P. (2007) Bedrock channel adjustment to tectonic forcing: Implications for predicting river incision rates. *Geology*, v.35(2), pp.103-106.
- Wobus, C., Whipple, K.X., Kirby, E., Snyder, N., Johnson, J., Spyropoulou, K., Crosby, B., Sheehan, D. and Willett, S.D. (2006) Tectonics from topography: Procedures, promise, and pitfalls. *Special Papers, Geol. Soc. Amer.*, v.398, pp.55.
- Yasin, Q., Baklouti, S., Sohail, G.M., Asif, M. and Xufei, G. (2022) Evaluation of Neoproterozoic source rock potential in SE Pakistan and adjacent Bikaner-Nagaur Basin, India. *Sci. Rep.*, v.12(1), 11102.
- Zaprowski, B.J., Pazzaglia, F.J. and Evenson, E.B. (2005) Climatic influences on profile concavity and river incision. *Jour. Geophys. Res. Earth Surf.*, v.110(F3), pp.1-19.



**Mery Biswas** studied Geography and received Bachelors and Masters degrees in 2000 and 2002, respectively. Specialization: morphometry, NE Himalayan tectonics.



**Soumyajit Mukherjee** did B.Sc., M.Tech. and Ph.D. in (Applied) Geology in 1999, 2002 and 2007, respectively. Teaches structural geology and stratigraphy at present



**Adrija Raha** - Did BSc. and MSc. in Geography in 2017 and 2019, respectively. Presently working as a Project Assistant in a DST-SERB sponsored project.



**Vinit Kotak** completed his BSc. and MSc. in Geology from K.J. Somaiya College of Science and Commerce in 2020 and 2022, respectively. Presently working as a geologist at Sohams Foundation Engineering Pvt. Ltd.